Archives of Mechanics • Archiwum Mechaniki Stosowanej • 29, 2, pp. 313-324, Warszawa 1977

The differential geometry of disclinations: wedge disclinations

M. J. MARCINKOWSKI (MARYLAND)

THE TECHNIQUES of differential geometry have been applied to the study of both perfect and imperfect wedge disclinations in simple cubic crystals. It is found that all disclinations act as terminal points for a wall of dislocations and that in the case of imperfect disclinations, this wall is also a grain boundary.

Metody geometrii różniczkowej zastosowano do badania doskonałych i niedoskonałych krawędzi dysklinacji w prostych sześciennych kryształach. Wykazano, że wszystkie dysklinacje działają jak punkty końcowe dla ściany dyslokacji i w przypadku dysklinacji niedoskonałych ściana ta jest również brzegiem ziarna.

Методы дифференциальной геометрии применены для исследования идеальных и неидеальных граней дисклинаций в простых кубических кристаллах. Показано, что все дисклинации действуют как конечные точки для стенки дислокации и в случае неидеальных дисклинаций эта стенка является тоже границей зерна.

1. Introduction

THE CLOSE relationship between disclinations and grain boundaries has already been demonstrated [1, 2, 3]. These analyses, however, were restricted to simple Euclidean geometric arguments relating the crystal lattice to the coincidence site lattice. It is anticipated that still more insight into this problem could be obtained by employing the techniques of differential geometry. Such has indeed been found to be the case with respect to the treatment of grain boundaries themselves [4]. The following presentation will therefore be devoted to formulating as well as interpreting the various tensor quantities associated with disclinations. For simplicity, the analysis will be restricted to wedge disclinations only.

2. Distortion tensor associated with a wedge disclination

Consider the perfect crystal shown in Fig. 1a. Edge dislocations can be introduced into it from both sides until they meet along the vertical dotted line. The common point of meeting is termed a coincidence site and is denoted by an open circle. The resultant configuration, shown in Fig. 1b, is termed a negative 53.1° wedge disclination [2]. The wedge disclination obviously has associated with it both plastic and elastic strains. However, the elastic strains can be removed by cutting the configuration of Fig. 1b into two pieces along the vertical dotted line and allowing both to relax as shown in Fig. 1c or, alternatively, as shown in Fig. 1d. KONDO [5] has termed this process of dissection perfect tearing. Next,

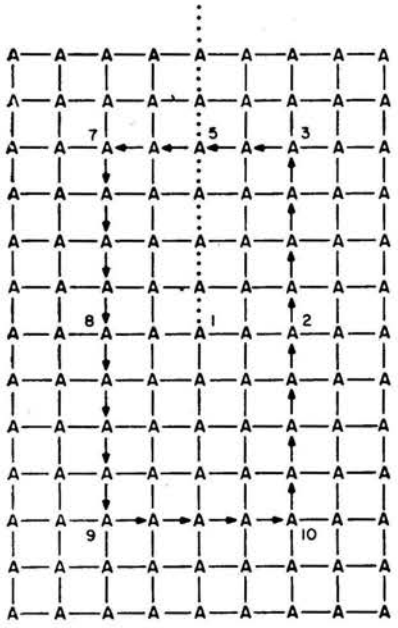

FIG. 1a. Initial state or perfect crystal lattice.

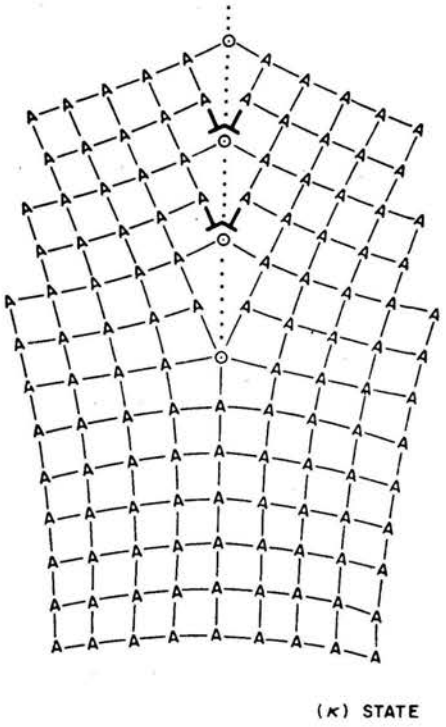

FIG. 1b. Final state or disclinated crystal lattice.

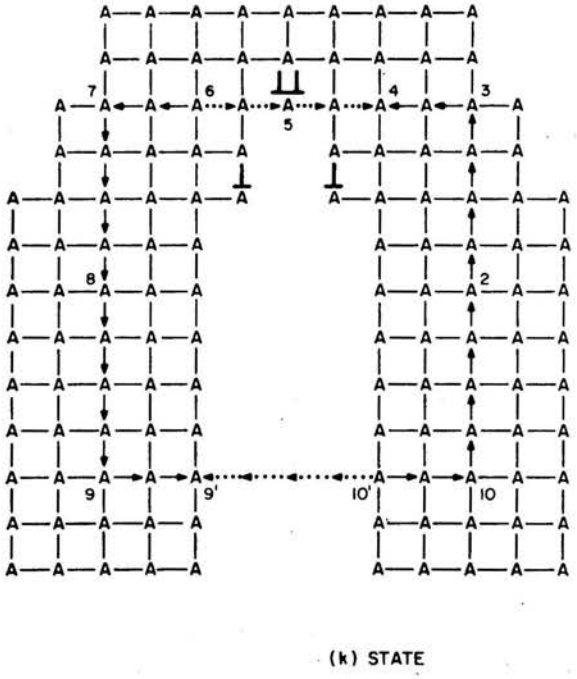

FIG. 1c. Natural state of disclinated crystal shown in Fig. 1b.

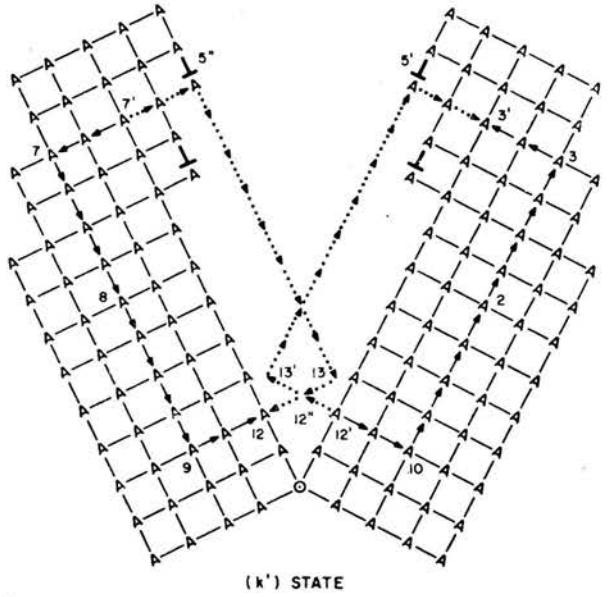

FIG. 1d. Alternate natural state of disclinated crystal in Fig. 1b.

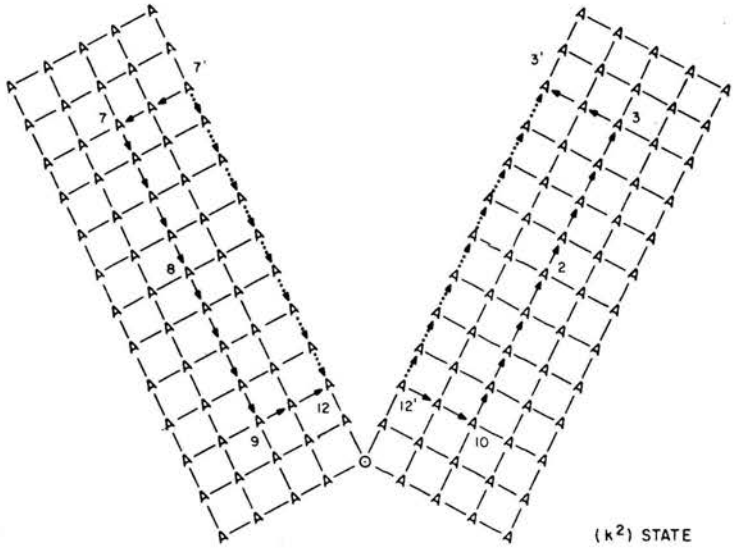

FIG. 1e. Anholonomic state of the perfect crystal shown in Fig. 1a.

it is convenient to refer to Figs. 1a and 1b as the initial and final states respectively and to Figs. 1c and 1d as natural states. These states will be designated by upper case Latin (K, L, etc.), lower case Greek ($\varkappa$, λ, etc.) and lower case Latin (k, l, etc.) superscripts and subscripts respectively. An additional numerical superscript will be used to differentiate the various natural states from one another, i.e. k^2, k^3, etc.

The local base vectors $\mathbf{e}_K$, $\mathbf{e}_\varkappa$ and $\mathbf{e}_k$, as well as the corresponding differential elements of length dx^K, $dx^\varkappa$ and dx^k, associated with the initial, final and intermediate states can all be related to one another by a set of distortion tensors as follows [6]:

$$\mathbf{e}_\varkappa = A^K_\varkappa \mathbf{e}_K, \qquad \mathbf{e}_K = A^\varkappa_K \mathbf{e}_\varkappa, \tag{2.1}$$

etc., while

$$dx^\varkappa = A^\varkappa_K dx^K, \qquad dx^K = A^K_\varkappa dx^\varkappa, \tag{2.2}$$

where the distortions are in turn related to one another by

$$A^\varkappa_K A^K_\lambda = \delta^\varkappa_\lambda, \qquad A^K_\varkappa A^\varkappa_L = \delta^K_L \tag{2.3}$$

etc. where δ^K_λ etc. are the Kronecker deltas. It is important to note that the torn pieces associated with the natural state are, in general, free to rotate and undergo translations. The distortions $A^\varkappa_k$, $A^k_\varkappa$, A^K_k and A^k_K are thus indeterminate with respect to the natural state. More generally, the natural state may be referred to as an anholonomic state. It is the uncertainty in the position of the torn pieces which makes the (k) state anholonomic [7]. If the orientation of the individual pieces, i.e. the distortions, are fixed in space as in the case of Figs. 1c or 1d, the space may be referred to as a natural anholonomic frame which possesses distant parallelism.

3. Metric and strain tensors

The following lengths dS can be associated with the three states shown in Fig. 1,

$$\underset{K}{dS^2} = g_{KL} dx^K dx^L, \qquad \underset{\varkappa}{dS^2} = g_{\varkappa\lambda} dx^\varkappa dx^\lambda, \qquad \underset{k}{dS^2} = g_{kl} dx^k dx^l, \tag{3.1}$$

where g_{KL}, $g_{\varkappa\lambda}$ and g_{kl} are metric tensors defined by

$$g_{KL} = e_K \cdot e_L, \qquad g_{\varkappa\lambda} = e_\varkappa \cdot e_\lambda \tag{3.2}$$

etc. [8]. The various g_{KL} are in turn related to one another by

$$g_{kl} = A^\varkappa_k A^\lambda_l g_{\varkappa\lambda}, \qquad g_{kl} = A^K_k A^L_l g_{KL} \tag{3.3}$$

etc. Furthermore, since the (K) state is Cartesian

$$g_{KL} = \delta_{KL} \tag{3.4}$$

whereas from Eq. $(3.3)_2$

$$g_{kl} = \delta_{kl} \tag{3.4'}$$

since the A_k^K represent rigid rotations. Eqs. (3.4) simply mean that the units of length are identical in both the initial and natural states which are of course elastically unstrained.

It is also instructive to define a set of three strain tensors as follows [6, 9]:

$$\begin{aligned} dS^2 - dS^2 &= 2\overset{T}{\varepsilon}_{\kappa\lambda} dx^\kappa dx^\lambda, \\ dS^2 - dS^2 &= 2\overset{E}{\varepsilon}_{\kappa\lambda} dx^\kappa dx^\lambda, \\ dS^2 - dS^2 &= 2\overset{P}{\varepsilon}_{\kappa\lambda} dx^\kappa dx^\lambda, \end{aligned} \tag{3.5}$$

where $\overset{T}{\varepsilon}_{\kappa\lambda}$, $\overset{E}{\varepsilon}_{\kappa\lambda}$ and $\overset{P}{\varepsilon}_{\kappa\lambda}$ are the total, elastic and plastic strain tensors respectively, associated with the disclination in Fig. 1. In particular, they are given by

$$\begin{aligned} \overset{T}{\varepsilon}_{\kappa\lambda} &= [g_{\kappa\lambda} - g_{\kappa\lambda}]/2, \\ \overset{E}{\varepsilon}_{\kappa\lambda} &= [g_{\kappa\lambda} - g_{\kappa\lambda}]/2, \\ \overset{P}{\varepsilon}_{\kappa\lambda} &= [g_{\kappa\lambda} - g_{\kappa\lambda}]/2. \end{aligned} \tag{3.6}$$

It is important to note that Eqs. (3.4) do not mean that Eq. $(3.6)_1$ vanishes. This arises from the fact that the (K) and (k) states have different external shapes, and that Eqs. (3.4) hold only within the interiors of the crystals, which cannot be everywhere coincident.

4. Affine connection, torsion tensor and anholonomic object

A vector c^λ which moves through a distance dx^μ undergoes a parallel displacement given by [10]:

$$dc^\varkappa = -\Gamma^\varkappa_{\mu\lambda} c^\lambda dx^\mu. \tag{4.1}$$

The quantity $\Gamma^\varkappa_{\mu\lambda}$ is termed the connection and in generalized, i.e. L_n type space, is defined as follows:

$$\Gamma^\varkappa_{\mu\lambda} = \left\{ \begin{matrix} \varkappa \\ \mu\lambda \end{matrix} \right\} + (S_{\mu\lambda}{}^\varkappa - S_{\lambda\cdot\mu}^{\ \ \varkappa} + S_{\cdot\mu\lambda}^{\ \ \varkappa}), \tag{4.2}$$

where the $\left\{ \begin{matrix} \varkappa \\ \mu\lambda \end{matrix} \right\}$ are Christoffel symbols of the second kind. The quantity $S_{\mu\lambda}{}^\varkappa$ is termed the torsion tensor which, from Eq. (4.2), is given by

$$S_{\mu\lambda}{}^\varkappa = \Gamma^\varkappa_{[\mu\lambda]}. \tag{4.3}$$

In those cases where the following condition holds

$$\Gamma^{k_2}_{m_2 l_2} = -A^K_{l_2} \partial_{m_2} A^{k_2}_K \tag{4.4}$$

or equivalently

$$\Gamma^{k^2}_{m^2 l^2} = A^{k^2}_K \partial_{m^2} A^K_{l^2}, \tag{4.4'}$$

we can write

$$\Gamma^{k^2}_{[m^2 l^2]} = -A^K_{m^2} A^L_{l^2} \partial_{[K} A^{k^2}_{L]} = -\Omega_{\dot{m}^2 \dot{l}^2}{}^{k^2} \tag{4.5}$$

or equivalently

$$\Gamma^{k^2}_{[m^2 l^2]} = A^{k^2}_K \partial_{[m^2} A^K_{l^2]}, \tag{4.5'}$$

where the quantity $\Omega_{\dot{m}^2 \dot{l}^2}{}^{k^2}$ is termed the anholonomic object. The conditions given by Eqs. (4.4) obtain when a quantity $R_{\dot{m}^2 \dot{l}^2 \dot{n}^2}{}^{k^2}$, termed the Riemann-Christoffel curvature tensor, given by [10]

$$R_{\dot{m}^2 \dot{l}^2 \dot{n}^2}{}^{k^2} = \partial_{m^2} \Gamma^{k^2}_{l^2 n^2} - \partial_{l^2} \Gamma^{k^2}_{m^2 n^2} + \Gamma^{k^2}_{m^2 r^2} \Gamma^{r^2}_{l^2 m^2} - \Gamma^{k^2}_{l^2 r^2} \Gamma^{r^2}_{m^2 n^2} \tag{4.6}$$

vanishes [11]. Spaces in which $S_{\dot{m}\dot{l}}{}^k$ vanish are termed A_n for which we may write

$$\Gamma^{k^2}_{m^2 l^2} = \begin{Bmatrix} k_2 \\ m^2 l^2 \end{Bmatrix} + (-\Omega_{\dot{m}^2 \dot{l}^2}{}^{k^2} + \Omega_{\dot{l}^2 \cdot m^2}{}^{k^2} + \Omega^{k^2}_{\cdot \, m^2 l^2}). \tag{4.7}$$

Such is the case for the (k^2) state shown in Fig. 1e which was produced by tearing the perfect crystal shown in Fig. 1a.

For the natural or anholonomic states of the wedge disclination in Fig. 1, we may write [10, 12]

$$\Gamma_{\dot{m}\dot{l}}{}^k = \begin{Bmatrix} k \\ lm \end{Bmatrix} + [(S_{\dot{l}\dot{m}}{}^k - \Omega_{\dot{l}\dot{m}}{}^k) - (S_{\dot{m}\cdot\dot{l}}{}^k - \Omega_{\dot{m}\cdot\dot{l}}{}^k) + (S^k_{\cdot lm} - \Omega^k_{\cdot lm})]. \tag{4.8}$$

Two additional expressions which can be shown to hold for the (k) state are

$$\begin{aligned} S_{\dot{l}\dot{m}}{}^k &= A^k_\varkappa A^\mu_l A^\lambda_m \Gamma^\varkappa_{[\mu\lambda]}, \\ \Gamma^k_{[lm]} &= S_{\dot{l}\dot{m}}{}^k - \Omega_{\dot{l}\dot{m}}{}^k. \end{aligned} \tag{4.9}$$

As mentioned earlier, in the most general anholonomic case, the locations as well as the orientations of the torn pieces are arbitrary. However, when the orientations of the torn pieces are fixed in space, as in the manner shown in Fig. 1c and 1d, the values of A^k_λ are uniquely determined and we may write Eq. $(4.9)_1$ as

$$S_{\dot{l}\dot{m}}{}^k \overset{*}{=} A^k_\varkappa A^\mu_l A^\lambda_m \Gamma^\varkappa_{[\mu\lambda]} \tag{4.10}$$

where the symbol $\overset{*}{=}$ signifies that the relation holds only in a given coordinate system. Noting, similar to Eq. (4.5'), that we can also write

$$\Gamma^\varkappa_{[\mu\lambda]} = A^\varkappa_l \partial_{[\mu} A^l_{\lambda]} \tag{4.11}$$

and substituting into Eq. (4.10) gives

$$S_{\dot{l}\dot{m}}{}^k \overset{*}{=} A^\mu_l A^\lambda_m \delta^k_l \partial_{[\mu} A^l_{\lambda]} = A^\mu_l A^\lambda_m \partial_{[\mu} A^k_{\lambda]} = \Omega_{\dot{l}\dot{m}}{}^k. \tag{4.12}$$

This in turn means that Γ^k_{lm} in Eq. (4.8) becomes zero, which shows that such a space possesses distant parallelism since $R_{\dot{l}\dot{m}\dot{o}}{}^k$, given by an expression of the form shown by Eq. (4.6), also vanishes. Thus, the anholonomic configuration of Fig. 1c and 1d having associated with them unique values of A^k_λ, possess distant parallelism.

5. Burgers circuit associated with a wedge disclination

The wedge disclination shown in Fig. 1b is reproduced again in Fig. 2 where a number of different Burgers circuits are drawn about and in the vicinity of the disclination whose core coincides with the lowermost coincidence point labeled as 1. Four specific Burgers circuits are considered and these are shown again in detail in Figs. 3a, 3b, 3c, and 3d. It is apparent that the circuits in Figs. 3a and 3c pass just outside, i.e. exclude the disclination core, while those in Figs. 3b and 3d pass just inside, i.e. include the disclination core.

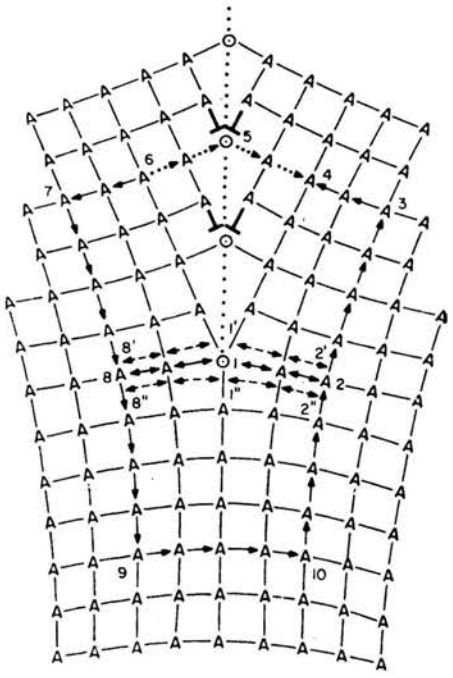

FIG. 2. Construction of various Burgers circuits around and in the vicinity of the wedge disclinations shown in Fig. 1b.

It is obvious that the unprimed drawings in Fig. 3 contain elastic strains. These may be removed as shown by the rightmost column or primed drawings in Fig. 3. In order for this relaxation to occur in the case of Figs. 3b′ and 3d′, the circuits which encompass the disclination had first to be cut at the points labeled 5 and 12 in Figs. 3b, and 3d, respectively. Such cutting was not necessary in the case Figs. 3a′ and 3c′ where the Burgers circuit did not encompass the disclination.

Close inspection of Figs. 3b′ and 3d′ show that they are simply special cases of the natural states shown in Figs. 1c and 1d, respectively. In particular, when the circuits in Figs. 3b′ and 3d′ are cut at points 1″ and 1′, respectively and rigidly translated by the required amounts, they can be mapped into, i.e., correspond to the states shown in Figs. 1c and 1d, respectively. Since this translation operation is mathematically trivial, the states shown in Figs. 1c and 3b′ as well as 1d and 3d′ are equivalent. Having made this connection we are now in a position to discuss the meaning of these Burgers circuits in a more quantitative manner.

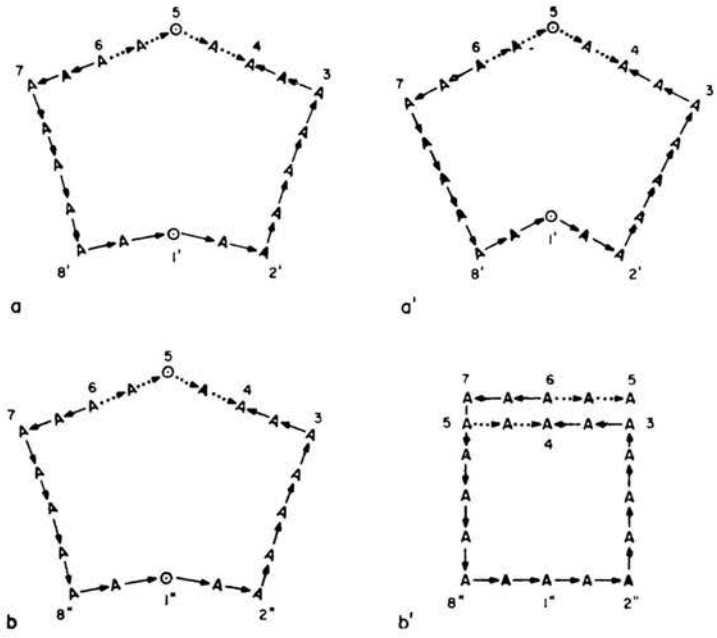

FIG. 3ab. Elucidation of the Burgers circuits shown in Fig. 2. Unrelaxed states denoted by a) and b). Relaxed states denoted by a′) and b′).

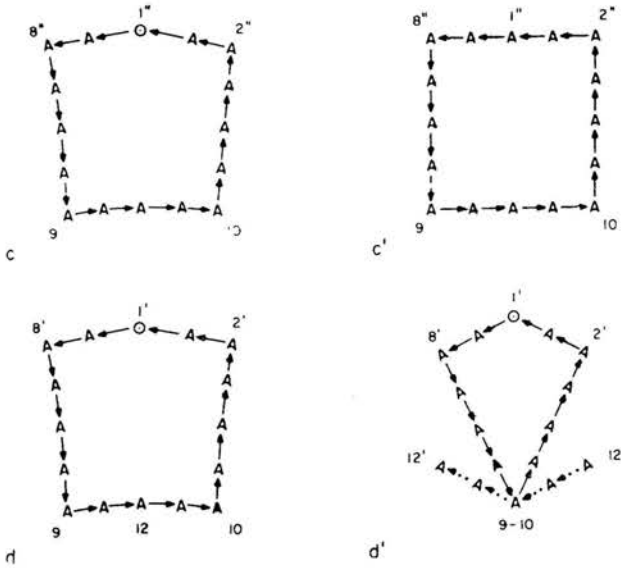

FIG. 3cd. Unrelaxed states denoted by c) and d). Relaxed states denoted by c′) and d′).

Consider, in particular, the Burgers circuits associated with the natural state (k) in Fig. 1c, which also corresponds to the circuit 2-3-5-7-8-9-10-2 associated with the initial state of Fig. 1a. This circuit is seen to contain closure failures of length 6-5-4 and 10′-9 which are shown by dotted arrows. The first of these closure failures is due to dislocations, while the second is due to the anholonomic object. Mathematically, the Burgers vector may be written in terms of the following surface integral:

$$b^k = -\int \Gamma^k_{[lm]} dF^{lm}, \tag{5.1}$$

where the integration is performed within the area outlined by the Burgers circuit. In view of Eq. (4.9), Eq. (5.1) becomes

$$b^k = -\int_S (S_{lm}{}^k - \Omega_{lm}{}^k) dF^{lm} = 0 \tag{5.1′}$$

since the torsion is equal to the anholonomic object. In terms of Fig. 1c. this means that the closure failure due to dislocations, i.e. the line 6-5-4, just balances or compensates that due to the anholonomic object, i.e. the line 10′-9′. Thus it is now also apparent that the dotted vectors shown in Fig. 3b′ correspond only to the dislocation content of the Burgers circuit. Similar reasoning holds for the case of the (k^1) state of Fig. 1d, except that now the additional closure failures 5″-13 and 13′-5 correspond only to the creation of free surfaces, i.e. the anholonomic object.

In the case of the (k^2) state in Fig. 1e, the closure failure associated with the Burgers circuit may be written as

$$b^{k^2} = \int_S \Omega_{i^2 m^2}{}^{k^2} dF^{i^2 m^2} \tag{5.2}$$

since no dislocations are present for this natural state. The value of b^{k^2} is given by the lengths 7′-12 and 12′-3′. For a crystal possessing a Burgers circuit such as that given in Fig. 3a′, on the other hand, we may write

$$b^{k^3} = -\int_S S_{i^3 m^3}{}^{k^3} dF^{i^3 m^3}; \tag{5.3}$$

such a (k^3) state in which $\Omega_{i^3 m^3}{}^{k^3} = 0$ corresponds simply to a symmetric grain boundary [4]. The Burgers circuit shown in Fig. 3c′ is that associated with a perfect crystal, i.e. state (K), so that the torsion tensor and anholonomic object are both zero.

Finally, all of the circuits shown in Figs. 3a, 3b, 3c and 3d correspond to the same state ($\varkappa$) but taken about two different areas. In the case of Figs. 3a and 3b we may write

$$b^\varkappa = -\int_S S_{\mu\lambda}{}^\varkappa dF^{\mu\lambda}. \tag{5.4}$$

That there must be torsion, and thus dislocations, associated with the disclinated state ($\varkappa$) follows from Eqs. (4.10) and (4.3). On the other hand, $S_{\mu\lambda}{}^\varkappa$ associated with the areas shown in Figs. 3c and 3d is zero, while $\Omega_{\mu\lambda}{}^\varkappa$ is always zero for the ($\varkappa$) state.

6. Perfect wedge disclinations

Thus far the discussion has been confined to partial wedge disclinations. These may be defined as those in which the wedge angle is other than one of the rotational symmetry operations of the lattice, i.e. 90°, 180°, etc. In particular, we have thus far considered only the imperfect 53.1° disclination as shown in Fig. 2. On the other hand, Fig. 4 shows a perfect

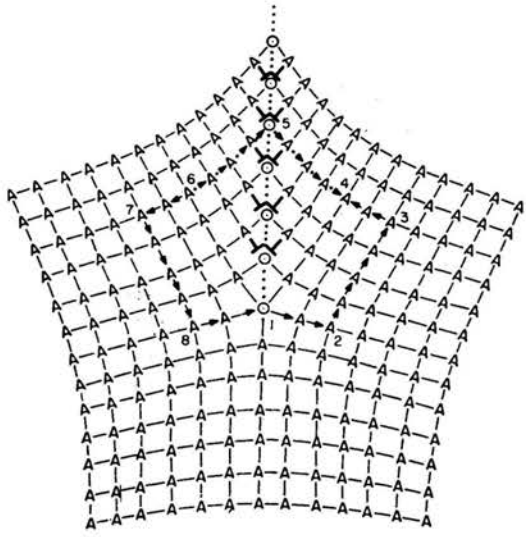

FIG. 4. Perfect negative 90° wedge disclination.

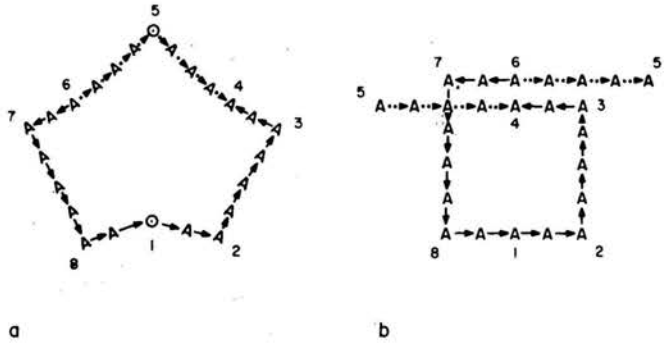

FIG. 5. Elucidation of the Burgers circuit shown in Fig. 4. Unrelaxed state denoted by a). Relaxed state denoted by b).

90° wedge disclination in a simple cubic lattice. As in the case of the partial disclination, an array of edge dislocations can be seen to terminate on the 90° disclination. However, unlike the partial disclination, the 90° disclination is seen to possess five-fold rotational symmetry so that the portrayal of the array of edge dislocations in Fig. 4 is not unique but may also be drawn at any one of the other four symmetry positions. That these are indeed real edge dislocations associated with the 90° disclination in spite of the deceptive

appearance of the lattice in Fig. 4, which seems almost perfect, can be seen by constructing a Burgers circuit along the path 1-2-3-4-5-6-7-8 in Fig. 4.

This circiuit is shown in greater detail in Fig. 5a. As in the case of the partial disclination, the circuit may be broken at point 5 and allowed to relax as shown in Figs. 5b. Fig. 5a and 5b thus refer to the final and natural states respectively, where it is obvious that the lengths 6-5 and 5-4 correspond to the eight edge dislocations enclosed by the Burgers circuit.

At this point the semantic question arises as to whether one should speak of grain boundaries terminating on perfect disclinations. We have already seen that dislocation walls terminate on all disclinations. However, the imperfect disclination is unique in that the wall has incorrect neighbour atoms associated with it, as in the case of the 53.1° disclination shown in Fig. 2, and is thus of relatively high energy. Furthermore, its position is unique in contrast to that found for the perfect disclination. It is these two specific features which perhaps enable us to describe a partial disclination as the terminus of a grain boundary.

7. Summary and conclusions

A detailed differential geometric analysis has been made with respect to the nature of disclinations. For simplicity, the analysis has been restricted to wedge disclinations in simple cubic crystals. Both partial and perfect disclinations have been considered in terms of several important tensor quantities including both torsion as well as curvature. Furthermore, the analysis has been made with respect to the deformed and natural (relaxed) states in which Burgers circuits have been constructed.

It has been shown that all disclinations can be viewed as the termini of a wall of dislocations and that in the case of partial disclinations this wall is also a grain boundary.

Acknowledgments

The present research effort was carried out at The Institut für Theoretische und Angewandte Physik der Universität Stuttgart in The Federal Republic of Germany under a Senior U.S. Scientist Award presented to the author by The Alexander von Humboldt Stiftung in conjunction with a one-year sabbatical leave. Financial support for this study was also provided in part by The National Science Foundation under Grant No. DMR-7202944. The author is indebted to Professor Ekkehart KRÖNER for his kind assistance during the course of this investigation, and to Professor K. SADANANDA of The Engineering Materials Group and The Department of Mechanical Engineering of The University of Maryland for his assistance with several of the disclination models.

References

1. M. J. MARCINKOWSKI and K. SADANANDA, Physica Status Solidi, **a18**, 361, 1973.
2. M. J. MARCINKOWSKI, E. S. P. DAS and K. SADANANDA, Physica Status Solidi, **a19**, 67, 1973.
3. K. SADANANDA and M. J. MARCINKOWSKI, Journal of Applied Physics, **45**, 1533, 1974.
4. M. J. MARCINKOWSKI, Acta Crystallographica, submitted for possible publication 1977.

5. K. KONDO, RAAG Memoirs, Vol. III. edited by K. KONDO, published by Gakujutsu Bunken Fukyu-kai, 173, 1962.
6. E. KRÖNER, Arch. for Rat. Mech. and Analys., 4, 273, 1959.
7. S. AMARI, RAAG Memoirs, Vol. III, edited by K. KONDO, published by Gakujutsu Bunken Fukyu-kai, Tokyo 100, 1962.
8. Y. C. FUNG, *Foundations of solid mechanics*, published by Prentice Hall, New Jersey 1965.
9. K. H. ANTHONY, *Fundamental aspects of dislocation theory*, edited by J. A. SIMMONS, R. DE WIT and R. BULLOUGH, NBS Special Publication No. 317, Washington, D. C., 1, 637, 1970.
10. J. A. SCHOUTEN, *Ricci-calculus*, published by Springer-Verlag, Berlin 1954.
11. E. SCHRÖDINGER, *Space-time structure*, published by Cambridge at the University Press 1954.
12. M. ŻÓRAWSKI, *Théorie mathématique des dislocations*, published by Dunod, Paris 1967.

DEPARTMENT OF MECHANICAL ENGINEERING
UNIVERSITY OF MARYLAND, MARYLAND, USA.

Received August 31, 1976.